

Scientific paper

# The Interaction of Acrolein with Pristine and N-doped TiO<sub>2</sub> Anatase Nanoparticles: A DFT Study

Amirali Abbasi<sup>1,2,3,\*</sup> and Jaber Jahanbin Sardroodi<sup>1,2,3</sup><sup>1</sup> Molecular Simulation laboratory (MSL), Azarbaijan Shahid Madani University, Tabriz, Iran<sup>2</sup> Computational Nanomaterials Research Group (CNRG), Azarbaijan Shahid Madani University, Tabriz, Iran<sup>3</sup> Department of Chemistry, Faculty of Basic Sciences, Azarbaijan Shahid Madani University, Tabriz, Iran

\* Corresponding author: E-mail: a\_abbasi@azaruniv.edu

Tel: +98-412-432-7541

Received: 16-02-2016

## Abstract

Density functional theory calculations were carried out in order to study the effects of the adsorption of acrolein molecule on the structural and electronic properties of TiO<sub>2</sub> anatase nanoparticles. The ability of pristine and N-doped TiO<sub>2</sub> anatase nanoparticles to recognize toxic acrolein (C<sub>3</sub>H<sub>4</sub>O) molecule was surveyed in detail. It was concluded that acrolein molecule chemisorbs on the N-doped anatase nanoparticles with large adsorption energy and small distance with respect to the nanoparticle. The results indicate that the adsorption of acrolein on the N-doped TiO<sub>2</sub> is energetically more favorable than the adsorption on the pristine one, suggesting that the N doping can energetically facilitate the adsorption of acrolein on the N-doped nanoparticle. It means that the N-doped TiO<sub>2</sub> nanoparticle can react with acrolein molecule more efficiently. The interaction between acrolein molecule and N-doped TiO<sub>2</sub> can induce substantial variations in the HOMO/LUMO molecular orbitals of the nanoparticle, changing its electrical conductivity which is helpful for developing novel sensor devices for the removal of harmful acrolein molecule. The large overlaps in the projected density of states spectra reveal the formation of chemical bond between two interacting atoms. Charge analysis based on Mulliken charges indicates that charge is transferred from the acrolein molecule to the TiO<sub>2</sub> nanoparticle.

**Keywords:** Acrolein; TiO<sub>2</sub>; Electronic properties; Density functional theory; sensor

## 1. Introduction

Titanium dioxide (TiO<sub>2</sub>) has been characterized as one of the most widely used photocatalytic materials with a wide range of applications in photo-catalysis,<sup>1</sup> gas sensor devices, heterogeneous catalysis and photovoltaic cells. It has attracted numerous scientific interests in the recent years because of its outstanding properties such as non-toxicity, chemical stability, abundance and high catalytic efficiency. These unique properties make TiO<sub>2</sub> very interesting material to be utilized in many fields of science and research.<sup>1–8</sup> Numerous attempts have been done in order to develop theoretical aspects of TiO<sub>2</sub> related science and technology including fundamental principles and crucial practical features of TiO<sub>2</sub>.<sup>1–15</sup> The photocatalytic activity of TiO<sub>2</sub> has been restricted due to its relatively wide band gap. This large band gap allows the absorption of the small percentage of the incoming solar light. One con-

venient solution to enhance the optical response and level of photo-efficiency of TiO<sub>2</sub> is non-metal doping such as nitrogen.<sup>16–18</sup> Several computational studies of N-doped TiO<sub>2</sub> nanoparticles have been published in the literature. For example, Liu et al. reported that the N doping can facilitate the adsorption of nitric oxide molecule on TiO<sub>2</sub> anatase nanoparticles.<sup>14</sup> Recently, it has been suggested that the N-doped TiO<sub>2</sub> anatase nanoparticles can react with CO molecules more efficiently, compared to the undoped ones.<sup>19</sup> Moreover, the nitrogen doping of TiO<sub>2</sub> nanoparticles improves its sensing capabilities, thus altering its electronic and structural properties.<sup>20–25</sup> The impacts of N-doping on the photo-catalytic activity and therefore the energy gap of TiO<sub>2</sub> have been inspected in some other works.<sup>26,27</sup> In order to reveal the enhancement of the efficiency of TiO<sub>2</sub> nanoparticles in the adsorption processes, some researchers have analyzed its electronic properties such as density of states (DOS), Mulliken population

analysis and also its structural properties such as bond lengths and adsorption energies.<sup>14,19,28</sup> A material in the atmosphere which causes harmful effects on the public health and the environment is identified as an air pollutant, which can have different forms such as solid particles, liquid droplets or gasses. Acrolein is in the liquid form and has been classified as a hazardous material.<sup>29</sup> It is produced as the result of incomplete combustion in the course of wood and house fires, plastics combustion, fast foods and mobile source emissions.  $C_3H_4O$  is mainly generated by cigarette smoking (50–90 ppm of  $C_3H_4O$  per cigarette). It can also make detrimental effects on the lung cells and can be also characterized as one of the most dangerous lung irritants.<sup>30</sup> Thus, the removal of  $C_3H_4O$  molecule from the atmosphere is an important subject to public health and environmental protection.<sup>31</sup> An admirable gas sensor should have some important properties such as high sensitivity to the harmful material, extensive variety of application and low price fabrication.<sup>32</sup> Solid state sensors such as  $TiO_2$  anatase nanoparticles are one of the most broadly used materials for recognition of toxic molecules in the atmosphere due to their unique response to the air pollutants. In this work, we have studied the adsorption behaviors of undoped and N-doped  $TiO_2$  anatase nanoparticles for chemical sensing of  $C_3H_4O$  molecule. We have considered different adsorption configurations of the  $C_3H_4O$  molecule on the  $TiO_2$  anatase nanoparticles. The variations of the structural and electronic properties of the considered nitrogen-doped  $TiO_2$  anatase nanoparticles resulting from the adsorption of  $C_3H_4O$  were studied in detail. Based on the obtained results, it can be concluded that the electronic properties of  $TiO_2$  anatase nanoparticle are strongly changed by the adsorption of  $C_3H_4O$ . This work aims to supply an overall understanding on the adsorption behaviors of  $TiO_2$  nanoparticles for the detection of harmful  $C_3H_4O$  molecule in the environment.

## 2. Details of Computations and Structural Models

### 2.1. Computational Methods

The calculations were performed based on DFT<sup>33,34</sup> as implemented in the Open source Package for Material eXplorer (OPENMX3.7),<sup>35</sup> which has been demonstrated to be an efficient software package for the simulation of large atomic systems. The same outer electrons of Ti atom were considered as valence electrons in the self-consistent field iterations. Pseudo atomic orbitals (PAOs) centered on atomic sites were used as basis sets in order to expand the wave functions in a KS scheme with a cutoff energy of 150 Ry (Rydberg).<sup>34</sup> The numerical PAO basis functions were generated by using a basis set of two-s, two-p, one-d for Ti atom, two-s and two-p for O, N and C atoms and two-s for H atom with the considered cutoff radii set to the

values of 7 for Ti, 5.5 for H and 5 for O, N and C (all in Bohrs). The generalized gradient approximation (GGA) in the Pedrew-Burke-Ernzerhof (PBE) form was used in order to describe the exchange-correlation energy functional.<sup>36</sup> An open-source program XcrysDen<sup>37</sup> was used for visualization of the data such as molecular orbitals and the other figures. All particles are separated by a vacuum space of about 11.5 Å, which has been tested and proven to avoid the interaction force between neighbor particles. Different adsorption configurations of  $C_3H_4O$  on  $TiO_2$  anatase nanoparticles are considered in this work. The configurations included both parallel and perpendicular orientations of the  $C_3H_4O$  molecule towards the pristine and N-doped nanoparticles. The adsorption energy was calculated by using the following formula:

$$E_{ad} = E_{(particle + adsorbate)} - E_{particle} - E_{adsorbate} \quad (1)$$

where  $E_{(particle + adsorbate)}$ ,  $E_{particle}$  and  $E_{adsorbate}$  are the total energies of the complex system,  $TiO_2$  nanoparticle without any adsorbed molecule and free  $C_3H_4O$  molecule in the vacuum, respectively. The charge transfer between the  $C_3H_4O$  molecule and the  $TiO_2$  nanoparticle was evaluated based on Mulliken charge analysis.

### 2.2. Structural Models

The studied  $TiO_2$  anatase nanoparticles were constructed by placing a  $3 \times 2 \times 1$  supercell of pristine and N-doped  $TiO_2$  anatase along x, y and z axes, respectively. The considered unit cell of  $TiO_2$  has been reported by Wyckoff, taken from “American Mineralogists Database”

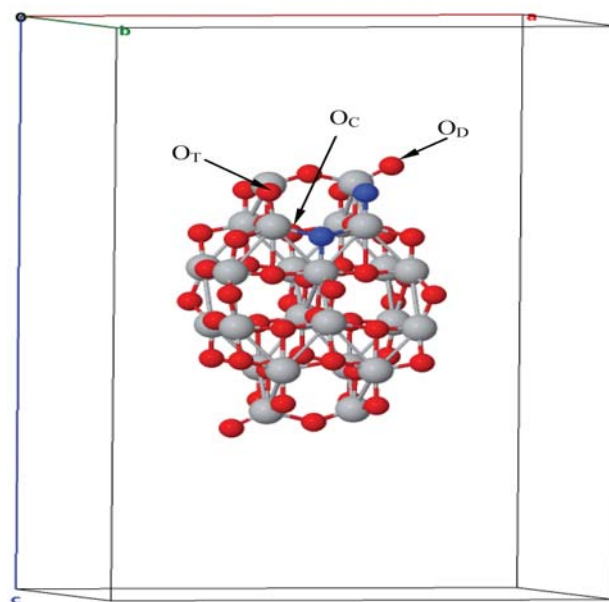


**Figure 1.** Optimized structure of the 72 atom N-doped  $TiO_2$  anatase nanoparticle constructed from  $3 \times 2 \times 1$  unit cells;  $O_C$ : central oxygen;  $O_T$ : twofold coordinated oxygen;  $O_D$ : dangling oxygen.

webpage.<sup>39</sup> Figure 1 displays the optimized structure of 2N-doped TiO<sub>2</sub> anatase located in an appropriate simulation box. The size of the studied nanoparticles has been chosen following Lei et al.<sup>11</sup> and Liu et al.<sup>14</sup>. The results published by Lei et al.<sup>11</sup> indicated that the smaller the particle is, the higher the average energy is. They have demonstrated that the 72 atom TiO<sub>2</sub> nanoparticles have the lowest energy among the different types of nanoparticles.

The size of the box considered in these calculations is 20 × 15 × 30 Å<sup>3</sup>, being larger than the size of the chosen nanoparticle. Two oxygen atoms of pristine TiO<sub>2</sub> (twofold coordinated and threefold coordinated oxygen atoms) were substituted by nitrogen atoms to build N-doped nanoparticles. Twofold coordinated and threefold oxygen atoms are denoted by O<sub>T</sub> and O<sub>C</sub> (middle oxygen), respectively (see figure 1). Acrolein (C<sub>3</sub>H<sub>4</sub>O) is the simplest unsaturated aldehyde with three carbon, four hydrogen and one oxygen atoms. The acrolein molecule is positioned parallel and perpendicular with respect to the optimized undoped and N-doped nanoparticles on different orientations. The optimization of the complex system shows that the oxygen atom of acrolein molecule preferentially interacts with the fivefold coordinated titanium atom of TiO<sub>2</sub>. This reveals a higher activity of oxygen atoms of acrolein, compared to the carbon atoms. The optimized structures of the N-doped nanoparticles were displayed in Figure 2.

### 3. Results and Discussion

#### 3.1. Bond Lengths and Adsorption Energies

The acrolein molecule was adsorbed on the fivefold coordinated Ti site of TiO<sub>2</sub>. In one orientation, acrolein molecule was placed vertically towards the nanoparticle (perpendicular orientation) and the other is that acrolein was put horizontally on the nanoparticle (parallel orienta-

tion). Figure 3 displays the optimized geometry configurations of TiO<sub>2</sub> nanoparticles with adsorbed acrolein molecules. This Figure includes the C<sub>3</sub>H<sub>4</sub>O-adsorbed complexes, labeled by A1-A5 for perpendicular configuration and A6-A9 for parallel one.

Each complex in Figure 3 differs in the substituted oxygen atom of TiO<sub>2</sub> nanoparticle and/or adsorbed C<sub>3</sub>H<sub>4</sub>O orientation from the other complexes. For example, complex A2 was constructed from N-doped TiO<sub>2</sub> (at O<sub>C</sub> site) and C<sub>3</sub>H<sub>4</sub>O molecule with perpendicular orientation. The optimized values of some bond lengths before and after the adsorption on the nanoparticle are listed in Table 1. The reported bond lengths in this table include the newly formed Ti-O bond and C-O bond of C<sub>3</sub>H<sub>4</sub>O molecule. The results indicate that the C-O bond of C<sub>3</sub>H<sub>4</sub>O molecule was elongated after the adsorption process. These variations of bond lengths are probably due to the transfer of electronic density from Ti-O<sub>D</sub> bond of TiO<sub>2</sub> and C-O bond of the adsorbed C<sub>3</sub>H<sub>4</sub>O molecule to the newly formed Ti-O bond between the titanium atom of TiO<sub>2</sub> nanoparticle and the oxygen atom of the C<sub>3</sub>H<sub>4</sub>O molecule. The smaller the bond formed between the oxygen atom of acrolein molecule and the titanium atom (Ti-O), the stronger the adsorption of acrolein on the TiO<sub>2</sub> anatase nanoparticle. The most stable adsorption configurations of the acrolein molecule on the undoped and N-doped TiO<sub>2</sub> nanoparticles are shown in Figure 3. The results of adsorption energies indicate that the acrolein molecule is preferentially adsorbed on the fivefold coordinated titanium site of TiO<sub>2</sub> through its oxygen atom. The calculated adsorption energies are listed in Table 1. These results indicate that the adsorption of C<sub>3</sub>H<sub>4</sub>O molecule on the N-doped nanoparticle is energetically more favorable than the adsorption on the undoped one. The small adsorption distance and great adsorption energy reveal chemisorption of acrolein molecule on the nanoparticles. The results also show that the O<sub>C</sub>-substituted nanoparticle adsorbs acrolein

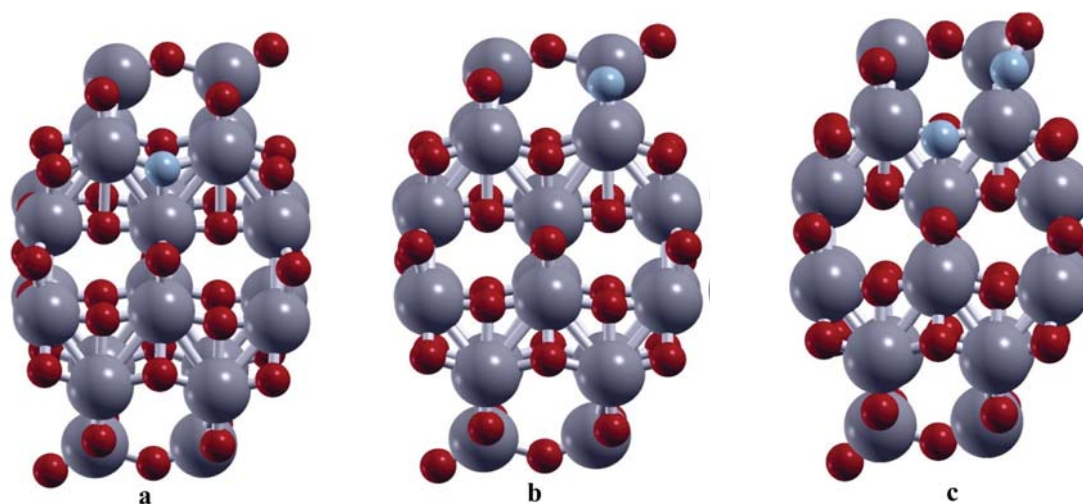


**Figure 2.** Optimized N-doped TiO<sub>2</sub> anatase nanoparticles, (a) O<sub>C</sub> substituted N-doped anatase nanoparticle, (b) O<sub>T</sub> substituted and (c) O<sub>C</sub>, T substituted one. The larger gray spheres are Ti atoms and the small red and blue ones represent O and N atoms, respectively.

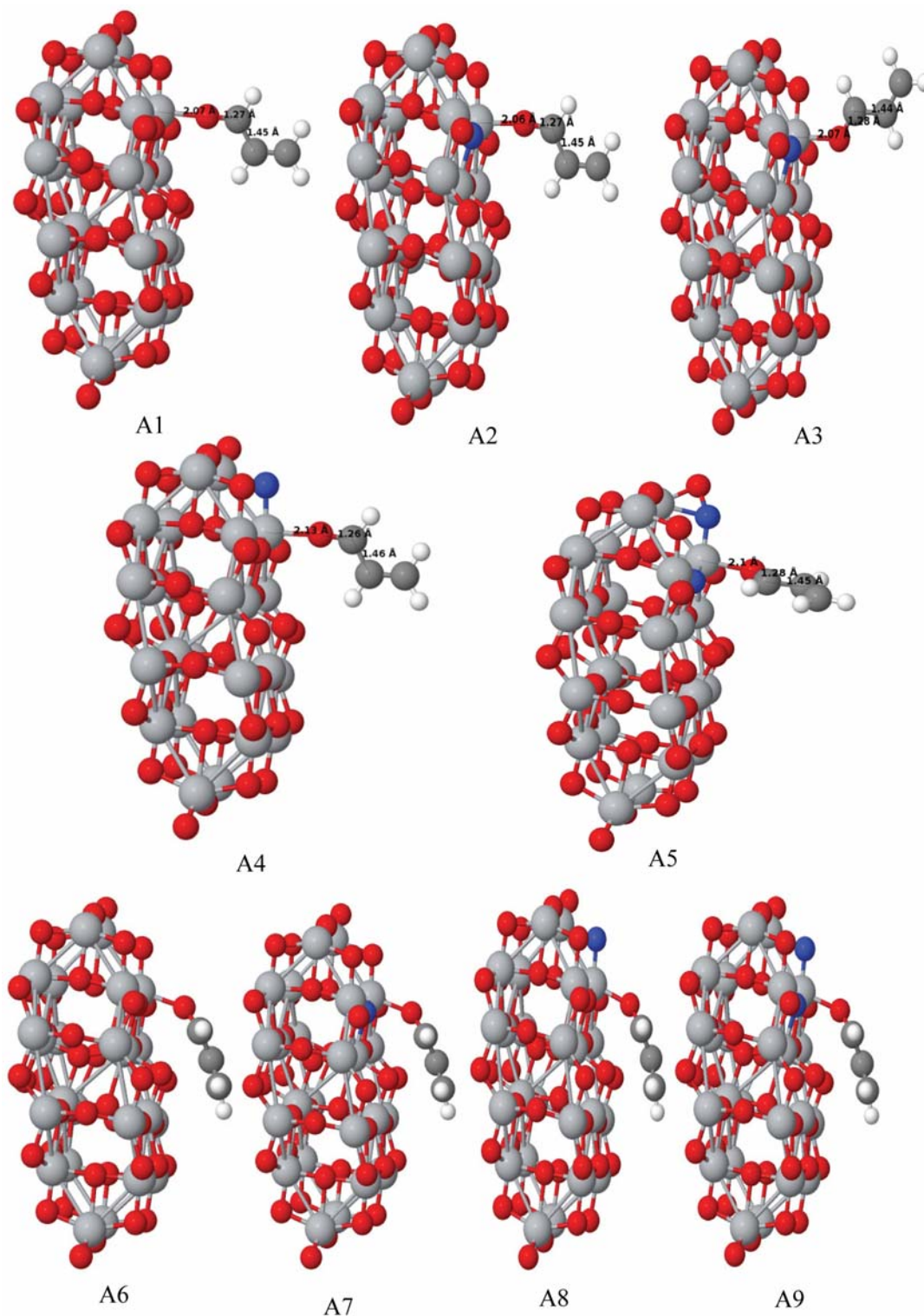


**Fig. 3.** Optimized geometry configurations of  $C_3H_4O$ - $TiO_2$  complexes. Colors represent atoms accordingly, Ti in light grey, O in red, N in blue, C in dark grey and H in white.

molecule more efficiently, compared to the  $O_T$ -substituted one. Besides, the adsorption on the 2N-doped nanoparticle was found to be more energetically favorable than the adsorption on the N-doped nanoparticle, suggesting that the

N-doping strengthens the adsorption of  $C_3H_4O$  on the  $TiO_2$  nanoparticle. In other words, two doped nitrogen atoms in the nanoparticle make the interaction of  $C_3H_4O$  molecule with  $TiO_2$  stronger. The more negative the adsorption ener-

gy, the higher tendency for adsorption, and consequently more energy favorable adsorption. The improvement of both adsorption energy and structural properties of the adsorption of  $C_3H_4O$  on  $TiO_2$  resulting from N-doping indicates that the N-doped  $TiO_2$  can be effectively used for the removal of the toxic acrolein molecules in the environment. The increasing of efficiency of the  $TiO_2$  nanoparticles in the adsorption process by N-doping has been recently studied by Liu et al. for adsorption of CO molecule.<sup>19</sup>

### 3. 2. Electronic Structures

**Figure S1** displays the total density of states (TDOS) for the pristine and the N-doped anatase  $TiO_2$  particles before and after the adsorption process. This Figure shows that the differences between DOS of doped and undoped  $TiO_2$  are increased by the adsorption of  $C_3H_4O$  molecule. These differences included both increa-

sing shifts of the energies of states and creation of some peaks in the DOS of the pristine  $TiO_2$ . The main changes are the creation of some small peaks in the DOS of N-doped  $TiO_2$  at the energy range of  $-7$  eV to  $-12$  eV. As distinct from the DOS spectra, the energies of the states were shifted to the lower values and also the energy gap of  $TiO_2$  was slightly downshifted (especially in panel d), implying that the conductivity of the system was improved upon  $C_3H_4O$  adsorption. This improved conductivity increases the sensing capability of  $TiO_2$  nanoparticles for  $C_3H_4O$  detection. The changes in DOS states would affect the electronic transport properties of the nanoparticles and this feature can be useful for sensing of  $C_3H_4O$  by  $TiO_2$  nanoparticles. The positive variations in the DOS of  $TiO_2$  around the Fermi level improves the sensitivity of the  $TiO_2$  for chemical sensing of  $C_3H_4O$ . The titanium and oxygen projected DOSs (Ti-PDOS and O-PDOS) were shown in Figure 4 (panels (a–f) for perpendicular adsorption con-

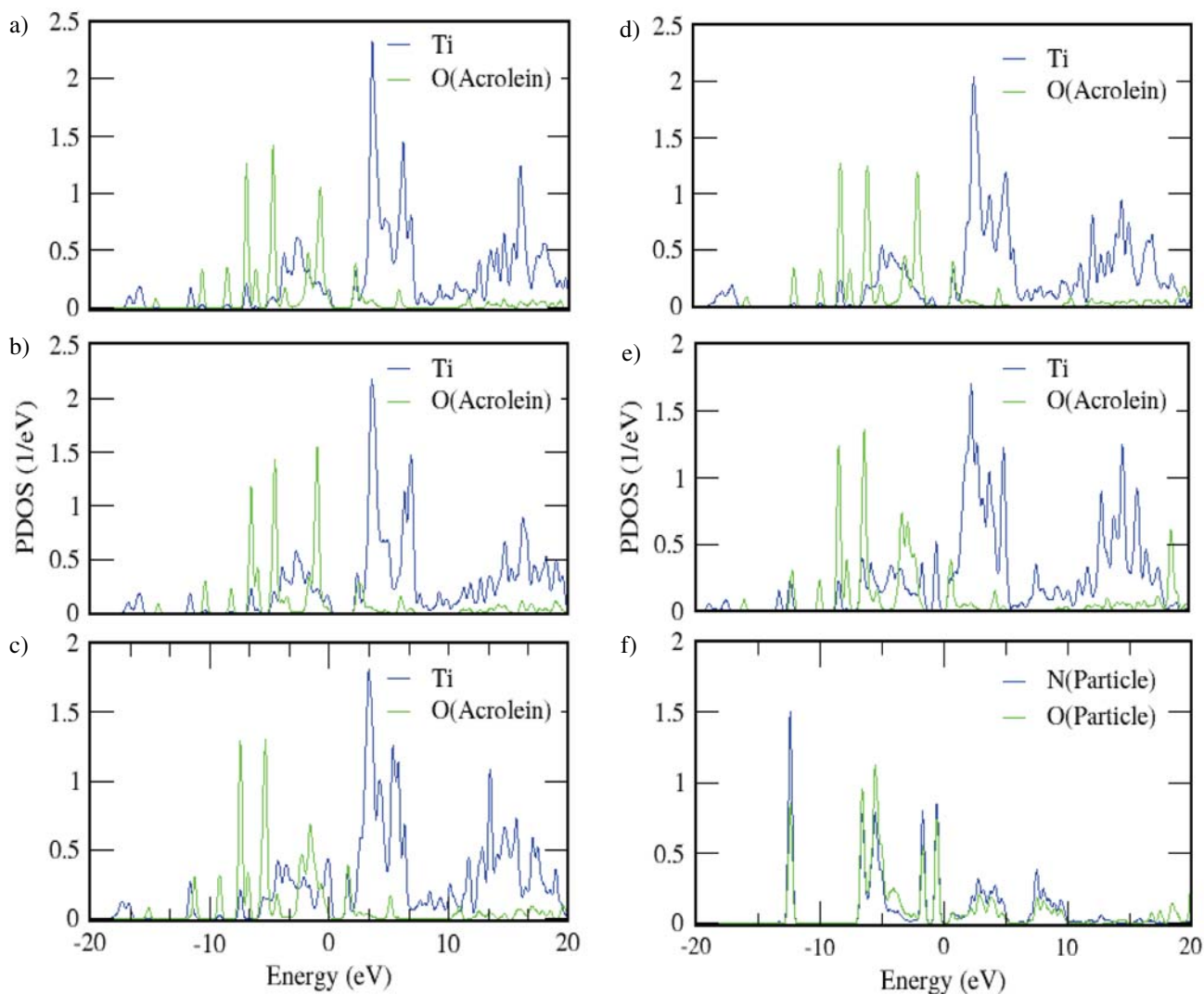


**Figure 4.** PDOS for the adsorption of  $C_3H_4O$  molecule on the N-doped nanoparticles, a: Complex A1; b: Complex A2; c: Complex A3; d: Complex A4; e: Complex A5; f: Complex A6.

figuration). The large overlaps between the PDOSs of these two atoms reveal the formation of new Ti-O bond between the titanium atom of nanoparticle and oxygen atom of acrolein molecule. This implies that the acrolein molecule chemisorbs on the  $\text{TiO}_2$  nanoparticle.

The corresponding PDOSs of the titanium and oxygen atoms for parallel configuration were shown in **Figure S2**, indicating considerable overlaps between the PDOSs of titanium and oxygen atoms. This PDOS overlaps represent that the oxygen atom of the acrolein molecule forms chemical bond with the fivefold coordinated titanium atom of  $\text{TiO}_2$ . For perpendicular configuration, the PDOSs of the titanium and oxygen atoms before and after the adsorption process were presented in **Figure S3**. This figure mainly shows the small shifts in the energy of the states to the lower energy values after the adsorption of acrolein molecule. The variations in the PDOS spectra are expected to make changes on the corresponding electronic properties. As a result, the chemisorbed acrolein on the N-

doped  $\text{TiO}_2$  gives rise to a considerable increase in the electrical conductivity of the doped  $\text{TiO}_2$  particle.

Figure 5 displays the isosurfaces of HOMO and LUMO molecular orbitals for acrolein molecule adsorbed on the nanoparticles. As a matter of convenience, we only presented the molecular orbital calculations for three complexes. These Figures show that the electronic densities in the HOMOs are mainly located on the acrolein molecule, whereas the LUMO's are strongly localized on the  $\text{TiO}_2$  nanoparticle. The increasing of the electronic density at the middle of the newly-formed bonds and consequently formation of new bonds were also confirmed by these molecular orbital diagrams.

### 3. 3. Charge Transfer Analysis

To further investigate the charge transfer between acrolein molecule and  $\text{TiO}_2$  nanoparticle, we present in Table 1 the charge analysis based on Mulliken charges for

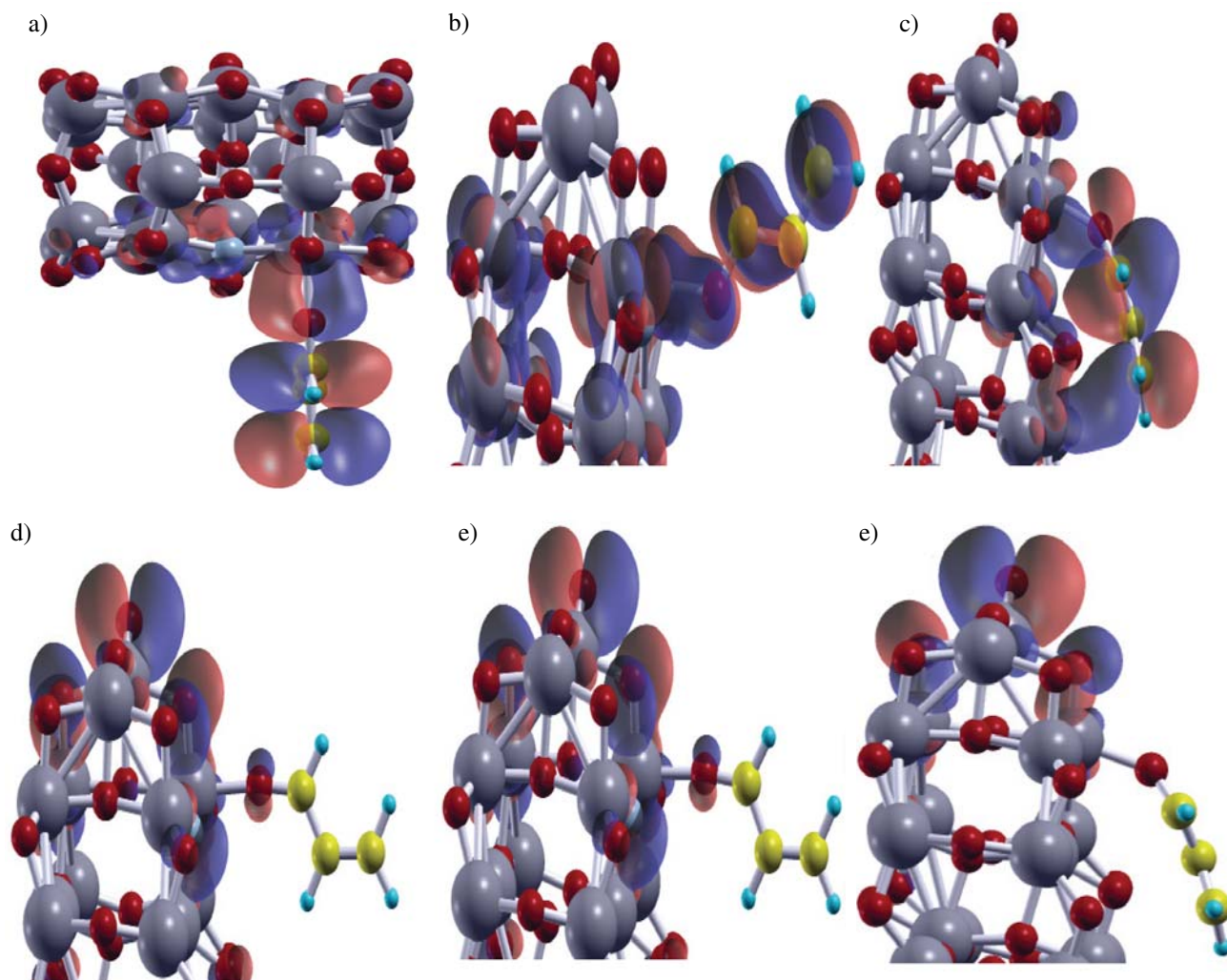


**Figure 5.** The isosurfaces of HOMO and LUMO molecular orbitals of the systems consisting of the  $\text{C}_3\text{H}_4\text{O}$  on the considered nanoparticles, a: Complex A2; b: Complex A1; c: Complex A6; d: Complex A2; e: Complex A1; f: Complex A6.

acrolein molecule. The charge difference for the particle  $j$  after and before adsorption, was calculated by using the following formula:

$$\Delta Q_j = Q_j(\text{in complex}) - Q_j(\text{in vacuum}) \quad (2)$$

where  $Q_j$  is the value of Mulliken charge of the  $j$ . Subscript “ $j$ ” means the  $\text{TiO}_2$  nanoparticle or acrolein molecule. The charge difference,  $\Delta Q_j$ , is a measure of the amount of charge transferred to, or, from the studied nanoparticles from, or, to the acrolein molecule. For configuration A1, the charge analysis reveals that acrolein adsorption induces a relatively considerable charge transfer of about  $-0.23 |e|$  ( $e$ , the electron charge) from acrolein to the  $\text{TiO}_2$  nanoparticle (see Table 1). It implies that  $\text{TiO}_2$  nano particle acts as an electron acceptor from the acrolein molecule. The  $\Delta Q$  values for other configurations are listed in Table 1. It should be noted that the charge transfer makes changes on the conductivity of the system. This could be an effective property to help in the design and improvement of  $\text{TiO}_2$ -based sensor devices for acrolein detection in the environment.

**Table 1.** Bond lengths (in Å), Mulliken charges (in  $|e|$ ) and adsorption energies (in eV) for a  $\text{C}_3\text{H}_4\text{O}$  molecule adsorbed on the  $\text{TiO}_2$  anatase nanoparticles.

Type of complex	Ti-O	C-O	$\Delta Q$	$\Delta E_{\text{ad}}$
A1	2.11	1.27	-0.23	-1.88
A2	2.20	1.25	-0.22	-3.58
A3	2.18	1.27	-0.27	-4.17
A4	2.13	1.26	-0.19	-3.17
A5	2.10	1.28	-0.27	-4.20
A6	2.10	1.28	-0.35	-1.48
A7	2.05	1.31	-0.38	-4.11
A8	2.06	1.25	-0.33	-3.95
A9	2.10	1.28	-0.35	-4.15
Non-adsorbed		1.23		

## 4. Conclusions

The adsorption behaviors of undoped and N-doped  $\text{TiO}_2$  anatase nanoparticles for acrolein detection were investigated using the DFT computations. We found that the N-doped nanoparticles have higher efficiency to adsorb toxic  $\text{C}_3\text{H}_4\text{O}$  molecule on their surfaces than the pristine ones. It means that the adsorption of  $\text{C}_3\text{H}_4\text{O}$  on the N-doped nanoparticles is more favorable in energy than the adsorption on the undoped ones. The effect of adsorption of  $\text{C}_3\text{H}_4\text{O}$  on the structural and electronic properties including the adsorption distances, adsorption energies, charge transfers, electronic DOS and PDOSs and molecular orbitals were calculated. It was found that N-doped  $\text{TiO}_2$  can be efficiently utilized for removing and sensing of  $\text{C}_3\text{H}_4\text{O}$  in the environment. Charge analysis based on Mulliken

charges indicates a charge transfer from acrolein molecule to nanoparticle. Adsorption of  $\text{C}_3\text{H}_4\text{O}$  molecule leads to significant changes in the electronic properties of  $\text{TiO}_2$  nanoparticle, altering its conductivity. Our calculated results present a great potential of N-doped  $\text{TiO}_2$  anatase for application as a highly sensitive molecule sensor.

## 5. Acknowledgement

This work has been supported by Azarbaijan Shahid Madani University.

## 6. Supplementary Material

DOS spectra for different adsorption configurations of acrolein molecule on the considered undoped and N-doped  $\text{TiO}_2$  nanoparticles and PDOS spectra for in order to reveal the overlap between interacting atoms.

## 7. References

- U. Diebold, *Surface Science Reports*, **2003**, *48*, 53–229. [http://dx.doi.org/10.1016/S0167-5729\(02\)00100-0](http://dx.doi.org/10.1016/S0167-5729(02)00100-0)
- F. Han, VSR. Kambala, M. Srinivasan, D. Rajarathnam, R. Naidu, *J. Applied Catalysis A: General*, **2009**, *359*, 25–40. <http://dx.doi.org/10.1016/j.apcata.2009.02.043>
- B. O'Regan, M. Gratzel, *Nature*, **1991**, *353*, 737–740. <http://dx.doi.org/10.1038/353737a0>
- D. J. Mowbray, J. I. Martinez, J. M. García Lastra, K. S. Thygesen, K. W. Jacobsen, *J. Phys. Chem. C.*, **2009**, *113*, 12301–12308. <http://dx.doi.org/10.1021/jp904672p>
- C. Zhang, P. J. D. Lindan, *J. Chemical Physics Letters*, **2003**, *373*, 15–21. [http://dx.doi.org/10.1016/S0009-2614\(03\)00530-X](http://dx.doi.org/10.1016/S0009-2614(03)00530-X)
- R. Erdogan, O. Ozbek, I. Onal, *J. Surface Science*, **2010**, *604*, 1029–1033. <http://dx.doi.org/10.1016/j.susc.2010.03.016>
- R. S. Armas, J. O. López, M. A. San-Miguel, F. Sanz, *J. Chem. Theory Comput.*, **2010**, *6* (9), 2856–2865. <http://dx.doi.org/10.1021/ct100289t>
- A. Abbasi, J. J. Sardroodi, *Int. J. Bio-Inorg. Hybr. Nanomater.*, **2016**, *5*(1), 43–52.
- A. Abbasi, J. J. Sardroodi, A. R. Ebrahimzadeh, *J. Water Environ. Nanotechnol.*, **2016**, *1*(1), 55–62.
- H. Zarei, M. Zeinali, H. Ghourchian, K. Eskandari, *Int. J. Nano. Dimens.*, **2013**, *4*(1), 69–75.
- Y. Lei, H. Liu, W. Xiao, *Modelling and Simulation in Materials Science and Engineering*, **2010**, *18*, 025004. <http://dx.doi.org/10.1088/0965-0393/18/2/025004>
- A. Beltràin, J. Andreis, J. R. Sambrano, E. Longo, *The Journal of Physical Chemistry A*, **2008**, *112*, 8943–8952.
- M. Mirzaei, H. Ahadi, M. Shariaty-Niassar, M. Akbari, *Int. J. Nanosci. Nanotechnol.*, **2015**, *11*(4), 289–295.

14. J. Liu, Q. Liu, P. Fang, C. Pan, W. Xiao, *J. Applied Surface Science*, **2012**, 258, 8312–8318.  
<http://dx.doi.org/10.1016/j.apsusc.2012.05.053>
15. A. Abbasi, J. J. Sardroodi, *Nanomed Res J.*, **2016**, 1(2), 69–78.
16. H. Irie, Y. Watanabe, K. Hashimoto, *Journal of Physical Chemistry B*, **2003**, 107(23), 5483–5486.  
<http://dx.doi.org/10.1021/jp030133h>
17. Y. Nakao, T. Morikawa, T. Ohwaki, Y. Taga, *J. Chemical Physics*, **2007**, 339, 20–26.
18. Q. Chen, C. Tang, G. Zheng, *J. Physica B: Condensed Matter*, **2009**, 404, 1074–1078.  
<http://dx.doi.org/10.1016/j.physb.2008.11.032>
19. J. Liu, L. Dong, W. Guo, T. Liang, W. Lai, *The Journal of Physical Chemistry C*, **2013**, 117, 13037–13044.  
<http://dx.doi.org/10.1021/jp4001972>
20. D. Zhao, X. Huang, B. Tian, S. Zhou, Y. Li, Z. Du, *Applied Physics Letters*, **2011**, 98, 115–124.
21. S. Livraghi, M. C. Paganini, E. Giamello, A. Selloni, C. Di Valentin, G. Pacchioni, *Journal of the American Chemical Society*, **2006**, 128(49), 15666–15671.  
<http://dx.doi.org/10.1021/ja064164c>
22. X. Q. Gong, A. Selloni, *J. Phys. Chem. B.*, **2005** 109 (42), 19560–19562. <http://dx.doi.org/10.1021/jp055311g>
23. C. Di Valentin, E. Finazzi, G. Pacchioni, A. Selloni, S. Livraghi, M. C. Paganini, E. Giamello, *J. Chemical Physics*, **2007**, 339, 44–56.
24. Y. Wang, D. J. Doren, *J. Solid State Communications*, **2005**, 136, 142–146.  
<http://dx.doi.org/10.1016/j.ssc.2005.07.014>
25. X. Han, G. Shao, *J. Phys. Chem. C.*, **2011**, 115, 8274.  
<http://dx.doi.org/10.1021/jp1106586>
26. H. Gao, J. Zhou, D. Dai, Y. Qu, *J. Chemical Engineering & Technology*, **2009**, 32, 867–872.  
<http://dx.doi.org/10.1002/ceat.200800624>
27. X. Cheng, X. Yu, Z. Xing, J. Wan, *J. Energy Procedia*, **2012**, 16, 598–605.  
<http://dx.doi.org/10.1016/j.egypro.2012.01.096>
28. M. Landmann, E. Rauls, W. G. Schmidt, *Journal of Physics: Condensed Matter*, **2012**, 24, 195503.  
<http://dx.doi.org/10.1088/0953-8984/24/19/195503>
29. I. Martínez, A. Ordóñez, J. Guerrero, S. Pedersen, A. Miñano, R. Teruel, L. Velázquez, S. R. Kristensen, V. Vicente, J. Corral, *FEBS Lett*, **2009**, 583(19), 3165–3170.  
<http://dx.doi.org/10.1016/j.febslet.2009.07.062>
30. J. Roy, P. Palapati, A. Betteieb, A. Tanel, D. A. Averill-Bates, *J. Chem Biol Interact*, **2009**, 181(2), 154–167.  
<http://dx.doi.org/10.1016/j.cbi.2009.07.001>
31. S. D. Sithu, S. Srivastava, M. A. Siddiqui, E. Vladykovskaya, D. W. Riggs, D. J. Conklin, P. Haberzettl, T. E. O'Toole, A. Bhatnagar, S. E. D'Souza, *Toxicol Appl Pharmacol*, **2010**, 248(2), 100–110.  
<http://dx.doi.org/10.1016/j.taap.2010.07.013>
32. Y. Sun, L. Chen, F. Zhang, D. Li, H. Pan, J. Ye, *Solid State Commun.*, **2010**, 150(39), 1906–1910.  
<http://dx.doi.org/10.1016/j.ssc.2010.07.037>
33. P. Hohenberg, W. Kohn, *J. Physical Review*, **1964**, 136, B864–B871 <http://dx.doi.org/10.1103/PhysRev.136.B864>
34. W. Kohn, L. Sham, *J. Physical Review*. **1965**, 140, A1133–A1138. <http://dx.doi.org/10.1103/PhysRev.140.A1133>
35. The code, OPENMX, pseudoatomic basis functions, and pseudopotentials are available on a web site 'http://www.openmxsquare.org'.
36. J. P. Perdew, K. Burke, M. Ernzerhof, *Physical Review Letters*. **1997**, 788, 1396.  
<http://dx.doi.org/10.1103/PhysRevLett.78.1396>
37. A. Koklj, *Comput. Mater. Sci.*, 2003, 28, 155–168.  
[http://dx.doi.org/10.1016/S0927-0256\(03\)00104-6](http://dx.doi.org/10.1016/S0927-0256(03)00104-6)
38. R. W. G. Wyckoff, crystal structures, Second edition. Interscience Publishers, USA, New York, **1963**.
39. Web page at: <http://rruff.geo.arizona.edu/AMS/amcsd>.

## Povzetek

Z uporabo funkcionalno gostotne teorije smo preučevali vplive adsorpcije molekule akroleina na strukturne in elektronske lastnosti čistih in N-dopiranih nanodelcev atanasa TiO<sub>2</sub>. Izkazalo se je, da se molekula akroleina z veliko energijo in majhno razdaljo kemisorbira na N-dopiranih nanodelcih anatasa. Adsorpcija akroleina na N-dopirani TiO<sub>2</sub> je energetsko ugodnejša od adsorpcije na čist TiO<sub>2</sub>, kar pomeni, da lahko N-dopirani TiO<sub>2</sub> nanodelci z molekulo akroleina učinkoviteje interagirajo. Interakcija med molekulao akroleina molekulo in N-dopiranim TiO<sub>2</sub> lahko povzroči znatne spremembe v HOMO/LUMO molekulskih orbitalah nanodelcev ter spremeni električno prevodnost sistema, kar je uporabno za razvoj novih senzorskih naprav za zaznavanje in odstranjevanje škodljivih molekul akroleina. Velika prekrivanja v gostoti napovedani stanj kažejo na možen nastanek kemijske vezi med dvema interagirajočima atomoma. Iz izvedene analize Mullikenovih nabojev lahko sklepamo na prenos naboja od molekule akroleina na nanodelec TiO<sub>2</sub>.